Lawrence Berkeley Laboratory
UNIVERSITY OF CALIFORNIA

Materials & Molecular Research Division

Submitted to the Journal of Chemical Physics

VIBRATION → VIBRATION ENERGY TRANSFER IN METHANE

Peter Hess, A. H. Kung, and C. Bradley Moore

November 1979

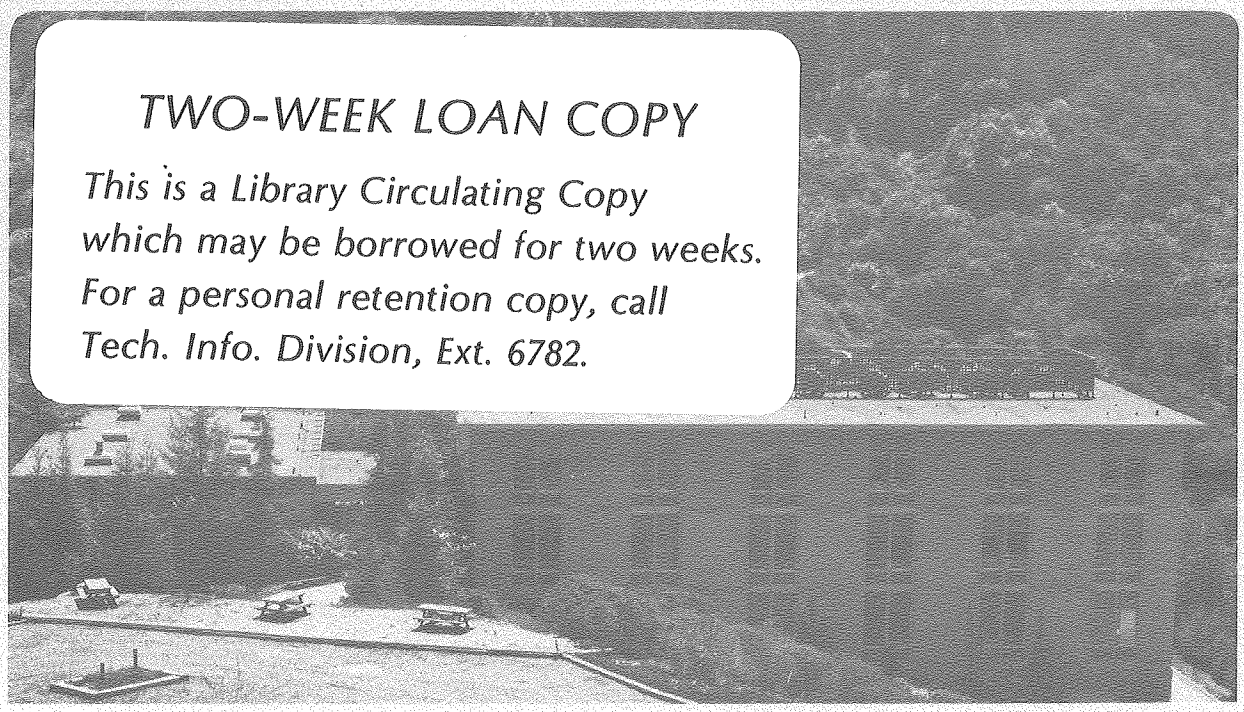

Prepared for the U.S. Department of Energy under Contract W-7405-ENG-48

DISCLAIMER

LBL 10060

Vibration → vibration energy transfer in methane

Peter Hess,[a] A.H. Kung, and C. Bradley Moore
Department of Chemistry, University of California,
and Materials and Molecular Research Division of
the Lawrence Berkeley Laboratory, Berkeley CA 94720

(Received)

Vibrational energy levels of methane in the range 2800 to 6000 cm^{-1} were excited by a pulsed tunable laser. Infrared fluorescence decays were observed at 294 K and analyzed to yield V → V energy transfer pathways and rates. Symmetric stretching excitation is converted to asymmetric stretching in the same molecule with a rate constant $k_1 = (3.6 \pm 0.9) \times 10^{-11}$ cm^3 $molecule^{-1}$ sec^{-1} (P = 0.09). The ν_2 and ν_4 bending vibrations are interconverted somewhat less rapidly. Stretching excitation is converted to bending with a rate constant of $(0.8 \pm 0.2) \times 10^{-11}$ cm^3 $molecule^{-1}$ sec^{-1} (P = 0.022) for the stretching fundamentals and about twice that for overtone or combination levels. The rate of almost exactly resonant transfer of a vibrational quantum from one molecule to another was about $(1.8 \pm 0.6) \times 10^{-11}$ cm^3 $molecule^{-1}$ sec^{-1} (P = 0.05) for transfer of a bending quantum from $CH_4(2\nu_4)$ and about three times less for transfer of a stretching quantum.

I. INTRODUCTION

Methane is a relatively simple polyatomic molecule whose structure and spectroscopy are well studied.[1] The presence of four fundamental vibrations makes the energy level diagram, Fig. 1, sufficiently complex that methane should be a useful prototype for understanding energy transfer processes in larger molecules. In many molecules CH stretching vibrations are clustered near 3000 cm^{-1} and bending vibrations in the 1200 - - 1500 cm^{-1} range.[2] The proximity of bending overtones and stretches provides a relaxation path which is undoubtedly important in most hydrocarbons.

In methane energy transfer among the vibrational modes, V → V transfer, is complete in a few microseconds at 1 Torr pressure.[3, 4] Vibrational deactivation to translation and rotation, V → T, R energy transfer, occurs only on the millisecond timescale at 1 Torr. V → T, R relaxation rates have been measured by many methods in pure methane and in mixtures with many other gases.[5 - 8] These results have helped to establish a good qualitative understanding of the role of rotation in vibrational relaxation. Laser-excited vibrational fluorescence experiments have given rates for V → V transfer between stretching and bending vibrations.[3, 4] Recent spectrophone data give some qualitative information on the overall mechanism of V → V transfer.[6, 7]

In this work a new powerful tunable ir laser system is used to excite a variety of combination and overtone levels as

well as the fundamental asymmetric stretching level in the 2800 to 6000 cm^{-1} range. Emission is monitored from both infrared active modes. Hot fluorescence (originating on combination and overtone levels) is distinguished from fundamental fluorescence. There are too many levels even in methane for a complete determination of rate constants coupling each possible initial and final vibrational level. However, rates are determined for the various types of V → V transfer processes and overall relaxation pathways are mapped in a general way.

II. EXPERIMENTAL

The basic experimental method has been descrived previously.[4, 9, 10] However, a new much more powerful tunable ir laser was developed for this work. A Raytheon model SS-404 Nd-YAG laser was used to pump an angle-tuned $LiNbO_3$ parametric oscillator (OPO). The master oscillator of the Nd:YAG laser is followed by three amplifiers. The bandwidth of the 1.06 μm pump beam was reduced by an etalon in the master oscillator. The Nd:YAG laser output consisted of pulses about 15 nsec in duration with energy limited to 190 - 200 mJ/pulse to avoid damage in the OPO. A repetition rate of 10 sec^{-1} was used in all experiments. The design of the OPO was similar to that described by Byer et al.[11] and utilised a grating and an etalon as line narrowing elements in the OPO cavity. This reduced the bandwidth of the OPO output to 0.15 cm^{-1}. The signal and idler waves of the OPO output were not separated because in all cases studied here only one of the two wavelengths was coincident with a CH_4 line. Typically, pulses with 3 mJ - 10 mJ were obtained depending on the pump power, the wavelength and whether the idler or the signal was used for excitation. To tune the OPO to desired wavelength the OPO output was reflected into a spectrometer. For fine tuning about 10% of the radiation was reflected into a spectrophone by a quartz beam splitter. The signal and idler were focused into the fluorescence cell, beam diameter one mm, and reflected back through this cell

into a pyroelectric detector which provided the trigger for the signal averaging system. In experiments with a low signal-to-noise the spectrophone was inserted between the fluorescence cell and the trigger detector. The infrared fluorescence was focused by a 5 cm diameter f/1 CaF_2 lens onto a Hg:Ge infrared detector cooled with liquid helium. To study hot fluorescence a 3.8 cm long gas filter cell containing 50, 150, 250 or 500 Torr CH_4 was placed between the fluorescence cell and the CaF_2 lens which focused fluorescence onto the detector. To block the scattered laser radiation three interference filters have been used in all experiments: one cooled inside the detector dewar and the other two external in front of the detector assembly. The preamplified detector signal was further amplified by a Keithley model 104 wideband amplifier and then averaged and recorded with an X-Y plotter. Depending on the line being excited several hundreds to 10,000 pulses were averaged. The signal-to-noise changed from better than 100-to-1 to only about 3 to 1 in two cases. The system response time was shorter than 300 nsec.

A Celesco pressure transducer was used to monitor the pressure in the fluorescence cell continuously. The errors introduced into the p_T values are less than 5% in the pressure range studied. The leak rate of the whole glass manifold including pressure gauge and fluorescence cell was below 10^{-3} Torr/h.

Matheson research-grade CH_4 was used without further purification (impurities in ppm: O_2 - 5, N_2 - 20, CO_2 - 50, C_2H_6 - 75, and C_3H_8 - 5). The $^{13}CH_4$ sample was provided by Stohler Isotope Chemicals and contained about 90% $^{13}CH_4$. $^{12}CH_4$ plus $^{13}CH_4$ were 98% - 99%. According to the manufacturer there are traces of air and CO. These impurities are far too dilute to affect measurements of the fast V → V rates described here. For accurate measurements of the much slower V → T, R rates these impurity levels are too high.[12]

III. RESULTS

A. ν_3 fluorescence

The ν_3 band at 3.3 μ is the strongest infrared-active fundamental of CH_4. In this work different bands were excited and the fluorescence from the ν_3 band observed. In the cases of $2\nu_3$, $\nu_3 + \nu_4$, and $\nu_1 + \nu_4$ excitation the interference filters were selected to transmit most of the ν_3 band fluorescence. Inside the detector dewar a broadband filter with 94% maximum transmission and half-transmission points at 2100 and 3150 cm^{-1} was used. At 2000 cm^{-1} and 3250 cm^{-1} the transmission of this filter was less than 1%. Two identical narrowband interference filters were placed outside the detector. These filters had 85% maximum transmission and half-transmission at 2915 - 3060 cm^{-1} and less than 1% outside 2780 - 3175 cm^{-1}. For excitation in the P-branch of the fundamental ν_3, fluorescence was observed only in the short wavelength part of the R-branch by using two narrowband interference filters. These had a maximum transmission of 57% and 83%, respectively, about half the maximum value at 3070 and 3205 cm^{-1} and less than 1% transmission outside the R-branch region. In the following subsections the results obtained by exciting different levels and observing the ν_3 fluorescence are described in detail.

Excitation of $2\nu_3$

The excitation of the overtone $2\nu_3$ was performed by

tuning the OPO signal wavelength to 6002.5 cm^{-1}, Q(6), and to 6077 cm^{-1}, R(6).[13] The relaxation time was independent of the rotational level excited. Hot ν_3 fluorescence was studied using the gas filter cell with 50 to 500 Torr CH_4. The data for 250 and 500 Torr CH_4 in the filter cell give the same rates as for pressures down to 50 Torr. The relaxation time derived from these data, Fig. 2, is 1.2 ± 0.3 μs Torr. Some experiments were performed without the filter cell. The $p\tau$ value found for the decay of the total ν_3 fluorescence was 2.3 ± 0.5 μs Torr. By subtracting the hot ν_3 fluorescence from the total ν_3 fluorescence a time of 3.3 ± 0.7 μs Torr, Fig. 2, was found for 1 → 0 relaxation of ν_3. Clearly the total fluorescence decays as the sum of at least two exponentials; thus the fit to a single decay time of 2.3 μsec Torr is meaningless.

Excitation of $\nu_3 + \nu_4$

Essentially the same experiments as for $2\nu_3$ were carried out for the combination band $\nu_3 + \nu_4$. The Q-branch of this band at 4313 cm^{-1} was excited. The $p\tau$ values for the fall of the hot and fundamental ν_3 fluorescence are the same within experimental error as those obtained for $2\nu_3$ excitation, Fig. 2.

Excitation of $\nu_1 + \nu_4$

For excitation of the Q-branch at 4216 cm^{-1} the ν_3 fluorescence decay times are the same as for $2\nu_3$ and $\nu_3 + \nu_4$,

Fig. 2. The amplitudes of hot and total ν_3 fluorescence extrapolated to t = 0 are the same within a 30% experimental uncertainty. A fluorescence rise time was observed in this case and could be analyzed in the pressure region below 1.5 Torr, Fig. 3. The $p\tau$ value for the rise of the hot ν_3 fluorescence is about 20% smaller than for the rise of the fundamental ν_3 fluorescence. The rise of the total ν_3 fluorescence is halfway between, $p\tau = 0.55 \pm 0.2$ μsec Torr.

Excitation of ν_3

Experiments carried out for P(9) and P(6) excitation at 2927 cm^{-1} and 2959 cm^{-1} respectively[14] gave the same relaxation time for the fall of ν_3 fluorescence, Fig. 4. This value of $p\tau = 3.2 \pm 0.6$ μsec Torr agrees with the values obtained before within the error limit.[4] Similar experiments performed with a sample containing approximately 90% $^{13}CH_4$ and 10% $^{12}CH_4$ lead to a slightly longer relaxation time, $p\tau = 3.5 \pm 0.6$ μsec Torr than for the normal CH_4 sample (see Fig. 4).

B. ν_4 fluorescence

The fundamental ν_3, the overtone $2\nu_3$ and the combination bands $\nu_1 + \nu_4$ and $\nu_2 + \nu_4$ were excited while ν_4 fluorescence was observed utilizing 3 interference filters. A long pass filter was used inside the detector with more than 85% transmission around 1300 cm^{-1}, half-transmission at 1950 cm^{-1} and less than 1% transmission beyond 2000 cm^{-1}. Outside the

detector a second long pass filter was inserted with more than 90% transmission around 1300 cm^{-1}, half-transmission point at 1510 cm^{-1}, and less than 1% transmission beyond 1590 cm^{-1}. In addition a wideband pass interference filter was employed outside the detector. This filter had between 80% and 90% transmission in the ν_4 band region, half-transmission at 1357 cm^{-1} and 853 cm^{-1}, and less than 1% transmission outside 820 cm^{-1} and 1410 cm^{-1}. In the following subsections the ν_4 fluorescence experiments performed with this filter combination are described in detail.

Excitation of ν_3

The Q-branch lines Q(3) and Q(4) of the ν_3 band were excited at 3018 cm^{-1}[14] with the OPO. Figure 5 shows the results obtained for the rise of the total ν_4 fluorescence. The $p\tau$ values derived from this figure are 3.2 ± 0.6 μsec Torr for the rise of the total ν_4 fluorescence. The signal-to-noise was about 50 in these experiments. The rise and fall of the hot ν_4 fluorescence were observed by using the CH_4 gas filter cell. Signal intensities are much weaker than for the total ν_4 fluorescence. In addition the fall of the hot ν_4 fluorescence did not return to the base line on the μsec timescale but rather on the msec timescale. Therefore, the uncertainty in the data analysis was much larger in this case than usual. In Fig. 5 the rise data are displayed. The approximate value determined from this figure is $p\tau$ = 1.8 ± 0.6 μsec Torr for the rise of the hot ν_4 fluorescence.

The fall data showed even larger scattering due to the base-line problem mentioned above and the low signal-to-noise ratio. Thus the fall time was set equal to the ν_3 fluorescence fall time in order to analyze for the rise times above.

Excitation of $\nu_2 + \nu_4$

This weak combination band was excited with the idler at 2825 cm^{-1}.[15] The best signal-to-noise achieved by averaging 5,000 to 10,000 shots was about 4, Fig. 6. The comparison of these data for the fall of the hot ν_4 fluorescence with the results for the rise of the hot ν_4 fluorescence exciting ν_3 in Fig. 5 shows that the relaxation time for these two processes is approximately the same ($p\tau$ = 1.8 ± 0.6 μsec Torr).

Excitation of $\nu_1 + \nu_4$

The Q-branch of the combination band $\nu_1 + \nu_4$ was excited at 4217 cm^{-1}. Part of the rise of the total ν_4 fluorescence was instantaneous in this case. By subtracting the hot ν_4 fluorescence from those traces the rise time of the fundamental ν_4 fluorescence was measured. This value agrees with the result obtained for the fall of the hot ν_4 fluorescence using the CH_4 gas cell between the fluorescence cell and detector. The $p\tau$ value for these two measurements is 3.0 ± 0.8 μsec Torr.

Excitation of $2\nu_3$

The lines Q(6) and R(6) were excited as in the ν_3

fluorescence experiments. The rise of the total ν_4 fluorescence was relatively slow and could therefore be investigated. The rise time was $p\tau = 1.5 \pm 0.3$ μsec Torr. Subtraction of the hot ν_4 fluorescence from the total ν_4 fluorescence leads to a $p\tau$ value of 3.0 ± 0.8 μsec Torr for the rise of the fundamental ν_4 fluorescence.

IV. DISCUSSION

The relaxation time data show that V → V energy transfer processes equilibrate all of the vibrational levels within a few microseconds at 1 Torr pressure. V → T, R relaxation of the equilibrated distribution, 82% $CH_4(\nu_4)$ and 18% $CH_4(\nu_2)$, occurs on a millisecond timescale at 1 Torr.[3, 8]

The multitude of overtone and combination levels and of energy transfer processes connecting them permits the determination of only a few rate constants for individual processes. The experimental data consist of intensity versus time for fluorescence from the ν_3 mode and from the ν_4 mode. The hot fluorescence from each of these modes gives the fraction of excitation in a mode which is associated with overtone and combination levels. In principle each fluorescence vs time curve may be decomposed into a sum of n exponentials where n is the total number of excited levels (Fig. 1) which are populated at some stage of the relaxation process. In practice because the V → V decay times are all of the same order of magnitude only one or two times may be determined from a given decay curve and many of these are identical within experimental error. Conclusions can be drawn regarding classes of processes and approximate rates for overall transfers from overtone and combination levels to fundamental levels and from one fundamental to another.

A. $\nu_1 \leftrightarrow \nu_3$ stretching equilibration

The most rapid energy transfer observed is the appearance of ν_3 fluorescence following excitation of $\nu_1 + \nu_4$. The only process which can lead to hot ν_3 is

$$CH_4(\nu_1+\nu_4) + M \xrightarrow{k_1} CH_4(\nu_3+\nu_4) + M - 98\ cm^{-1}. \quad (1)$$

$CH_4(\nu_3)$ may be produced subsequently by

$$CH_4(\nu_3+\nu_4) + CH_4 \xrightarrow{k_2} CH_4(\nu_4) + CH_4(\nu_3) - 4\ cm^{-1}, \quad (2)$$

or directly by

$$CH_4(\nu_1+\nu_4) + CH_4 \xrightarrow{k_3} CH_4(\nu_4) + CH_4(\nu_3) - 102\ cm^{-1}, \quad (3)$$

or by the sequence

$$CH_4(\nu_1+\nu_4) + CH_4 \xrightarrow{k_4} CH_4(\nu_1) + CH_4(\nu_4) + 1\ cm^{-1} \quad (4)$$

$$CH_4(\nu_1) + CH_4 \xrightarrow{k_5} CH_4(\nu_3) + CH_4 - 103\ cm^{-1} \quad (5)$$

Stretching energy may also be converted to two quanta of bending, $\nu_b = \nu_2$ or ν_4,

$$CH_4(\nu_1+\nu_4) + CH_4 \xrightarrow{k_6} CH_4((3-n)\nu_b) + CH_4(n\nu_b) \quad (6)$$

$$CH_4(\nu_1) + CH_4 \xrightarrow{k_7} CH_4((2-n)\nu_b) + CH_4(n\nu_b) \quad (7)$$

$$CH_4(\nu_3+\nu_4) + CH_4 \xrightarrow{k_8} CH_4((3-n)\nu_b) + CH_4(n\nu_b) \quad (8)$$

$$CH_4(\nu_3) + CH_4 \xrightarrow{k_9} CH_4((2-n)\nu_b) + CH_4(n\nu_b) \quad (9)$$

For completeness

$$CH_4(\nu_3+\nu_4) \xrightarrow{k_{10}} CH_4(\nu_1) + CH_4(\nu_4) + 99\ cm^{-1} \qquad (10)$$

should be considered.

Inspection of the rate equation for this system shows that the concentration of $CH_4(\nu_1+\nu_4)$ decays with the same rate constant, k_a, as for the rise of hot ν_3 fluorescence which all comes from $CH_4(\nu_3+\nu_4)$ by process (1). The loss of ν_1 quanta, $CH_4(\nu_1+\nu_4)$ and $CH_4(\nu_1)$ combined, and production of ν_3 quanta, $CH_4(\nu_3+\nu_4)$ and $CH_4(\nu_3)$combined, lead to a smaller rate constant for exponential rise in total ν_3 emission, $k_b = k_a - k_4$. Here it is assumed that $k_5 \approx k_1 + k_3$ and $k_6 - k_7 << k_a$. Figure 3 shows that k_a is greater than k_b by by roughly 5 - 15%. A generous allowance for systematic error due to self-absorption increases the range to 5 - 30%. Therefore

$$0.3\ k_a = 0.6\ \mu sec^{-1}\ Torr^{-1} \geq k_4 \geq 0.1\ \mu sec^{-1}\ Torr^{-1}.$$

The equal (± 25%) amplitudes of hot and total ν_3 fluorescence when extrapolated to t = 0 permit the conclusion, after allowing for possible self-absorption, that

$$k_1 > 3k_3.$$

The relative amplitude of ν_3 fluorescence excited through $\nu_1 + \nu_4$ and $\nu_3 + \nu_4$ normalized to the respective spectrophone signals were 1.0 ± 0.3 for hot fluorescence extrapolated to t = 0 and for both hot and total fluorescence for pressure · time ≈ 4 μsec Torr. Thus $\nu_1 + \nu_4$ equilibrates rapidly with

$\nu_3 + \nu_4$, process (1), before processes (3), (4) and (6) have proceeded significantly. Thus the ν_1 and ν_3 modes are equilibrated by collision-induced intermode transfer within the excited molecule at a rate fast compared to loss of stretching quanta or transfer from molecule to molecule. When the two stretching modes are equilibrated, 64% is ν_3 and 36% is ν_1. The rate constant $(k_1 + k_{-1}) = 1.56\ k_1$ is the rate constant for approach to this equilibrium. Thus $k_1 = k_b/1.56 = 1.2 \pm 0.3\ \mu sec^{-1}\ torr^{-1}$. Rate constants involving ν_3 on the reactants side which are for an equilibrated ν_3 and ν_1 mixture are denoted by a prime, e.g., $k_2' = 0.64(k_2+k_{10}) + 0.36(k_3+k_4)$. Since ν_3 and ν_1 products are not distinguished, both are included.

B. Stretch-to-bend deactivation

Deactivation of $CH_4(\nu_3)$ by energy transfer to the bending vibrations has been studied previously by exciting the fundamental band with a chopped He-Ne laser[3] and with a low power pulsed OPO.[4] Here a much higher power OPO is used. The original value for the relaxation time of 5.3 ± 0.8 μsec Torr is in reasonable agreement with the low power OPO value of 3.9 ± 0.6 μsec Torr. The still shorter value found here, 3.2 ± 0.6 μsec Torr, for excitation of the fundamental band may result from some heating by the laser or from the population of hot bands during the relaxation. The decay of "fundamental" fluorescence from overtone and combination excitations, 3.3 μsec Torr, can be distorted by subtracting

too much (τ too long) or too little (τ too short) hot fluorescence from the total. Notwithstanding these uncertainties, it can safely be concluded that the total rate of deactivation of $CH_4(\nu_3)$ to bending levels is

$$k_9' = 0.28 \pm 0.06\ \mu sec^{-1}\ Torr^{-1}.$$

The ν_4 fluorescence observed following the excitation of the ν_3 fundamental band was qualitatively the same as observed previously except that S/N was about five times larger. The rise time for hot ν_4 fluorescence is the same as the decay time discussed below for $2\nu_4$ in V → V equilibrium with $\nu_2 + \nu_4$. The decay of hot ν_4 fluorescence is fit well by the decay constant observed for the ν_3 fundamental fluorescence. However, the signal-to-noise is not high enough to make an accurate independent measurement of this decay time. The rise time for the total ν_4 fluorescence in previous studies[3, 4] was shorter than for the decay of ν_3 fluorescence. Here, however, the ν_3 fall and ν_4 rise are the same within the error margins. We have previously concluded that ν_3 was primarily relaxed by transfer to $2\nu_4$. All of our data remain consistent with this conclusion. However, the equilibration between ν_2 and ν_4 proceeds three to four times faster than the stretch bend relaxation and limits the possible difference between ν_3 fall and ν_4 rise. Furthermore, the possibility of systematic errors caused by self-absorption, by the difficulties of multiple exponential decay analyses, and perhaps, by other unidentified sources suggests

caution with respect to this conclusion.

Observations of ν_4 fluorescence following excitation of $2\nu_3$ and $\nu_3 + \nu_4$ give similar decay times to those discussed above. However, analysis of these results in terms of single and double exponentials does not give additional information on rate constants. There are just too many processes occuring simultaneously.

C. Relaxation of combination and overtone levels of ν_3

The excitation of $CH_4(2\nu_3)$ is followed by rapid equilibration of the ν_3 and ν_1 vibrations. At the lowest pressures the decay time was observed to be approximately the same as for the rise of ν_3 fluorescence following $\nu_1 + \nu_4$ excitation. The amplitude of this initial rapid decay was about 1/3 as expected from the 36% population of ν_1 when equilibrated with ν_3. Further relaxation may occur via the following processes,

$$CH_4(2\nu_3) + CH_4 \longrightarrow CH_4(\nu_3) + CH_4(\nu_3) - 33\ cm^{-1} \quad (11)$$

$$\longrightarrow CH_4(\nu_3+2\nu_b) + CH_4 \quad (12)$$

$$\longrightarrow CH_4(\nu_3+\nu_b) + CH_4(\nu_b) \quad (13)$$

$$\longrightarrow CH_4(\nu_3) + CH_4(2\nu_b) \quad (14)$$

$$CH_4(\nu_3+2\nu_b) + CH_4 \longrightarrow CH_4((4-n)\nu_b) + CH_4(n\nu_b) \quad (15)$$

$$\longrightarrow CH_4(\nu_3) + CH_4(2\nu_b) \quad (16)$$

and by process (9).

The small amplitude of the $\nu_3 = 1 \rightarrow 0$ "cold" fluorescence, 0.3 ± 0.15 of the total after $\nu_3 \leftrightarrow \nu_1$ equilibration, shows that processes (11) and (14) are less important than (12) and (13). The total rate of decay for hot ν_3 fluorescence following $CH_4(2\nu_3)$ excitation is 0.85 μsec^{-1} $Torr^{-1}$. The rate for transfer of a ν_3 quantum to bending for $CH_4(\nu_3)$ is 0.3 μsec^{-1} $Torr^{-1}$. The rate per quantum of ν_3 should be about the same for $CH_4(2\nu_3)$ and thus $k'_{12} + k'_{13} + k'_{14}$ might be about 0.6 μsec^{-1} $Torr^{-1}$. Since (14) requires not only conversion of stretching to bending but also transfer to another molecule, k'_{14} is probably much less than k'_{12}. The major process producing $CH_4(\nu_3)$ is probably (11). The product of total observed rate and fractional amplitude of "cold" ν_3 fluorescence gives,

$$k'_{11} + 2k'_{14} \simeq (0.85\ \mu sec^{-1}\ Torr^{-1}) \times 0.3 = 0.25 \pm 0.15\ \mu sec^{-1}\ Torr^{-1}.$$

Most of the stretching quanta are lost without production of $CH_4(\nu_3)$ via process (12) and perhaps (13) followed by (15). Thus

$$k_{12} + k_{13} = (0.85\ \mu sec^{-1}\ Torr^{-1}) \times 0.7 = 0.6 \pm 0.2\ \mu sec^{-1}\ Torr^{-1}.$$

The decays of ν_3 fluorescence following either $\nu_1 + \nu_4$ or $\nu_3 + \nu_4$ excitation give the same relaxation times. The decay of hot ν_3 fluorescence gives the total decay rate from $\nu_3 + \nu_4$,

$$k_c = k_2' + k_8' = 0.85 \pm 0.2 \quad \text{sec}^{-1}\ \text{Torr}^{-1}.$$

The fast initial decay due to equilibration between the ν_3 and ν_1 modes is not included in the analysis of the $\nu_3 + \nu_4$ results; rates are measured for the last half of the decay. The difference of less than 10% between the rates for $\nu_3 + \nu_4$ and $\nu_1 + \nu_4$, Fig. 4, is a measure of the systematic error involved.

Following $\nu_3 + \nu_4$ excitation and $\nu_1 \leftrightarrow \nu_3$ equilibration, excited state concentrations are

$$N_{\nu_3 + \nu_4} = N_0 \exp[-k_c t]$$

$$N_{\nu_3} = N_0 \frac{k_2}{k_2+k_8-k_9} \left\{ e^{-k_9 t} - e^{-k_c t} \right\}.$$

If Einstein A coeffficients are equal for ν_3 emission and if the filter transmissions are equal and there is no self absorption, then the fluorescence intensity ratios give the rate constant ratio $[k_2'/(k_2'+k_8'-k_9')]$. The total ν_3 fluorescence was analyzed as the sum of two exponentials with decay rate constants k_c and k_9. Since both decay constants are determined independently, the amplitude ratio was determined relatively well. In the pressure range 0.4 to 1 Torr it is constant at 0.25 ± 0.05. The constant ratio indicates that self-absorption is negligible below 1 Torr. However, some saturated absorption in the Q-branch may be possible. The true population amplitude ratio could be as high as 0.40.

The range 0.20 to 0.40 must be considered possible. The ratio k_2'/k_c is thus in the range 0.12 - 0.34 and $2.0 \leq k_8'/k_9' \leq 3.5$. Values for k_2' and k_8' are

$$0.1 < k_2' < 0.3 \ \mu sec^{-1} \ Torr^{-1}$$

$$k_8' = 0.7 \pm 0.2 \ \mu sec^{-1} \ Torr^{-1}.$$

Thus the $\nu_3 + \nu_4$ level is primarily relaxed by stretch-to-bend transfer rather than resonant intermolecular transfer. The rate of stretch-to-bend transfer is increased by about a factor of two for $\nu_3 + \nu_4$ compared to ν_3.

D. Nearly resonant transfers of bending quanta

The bending combination level $\nu_2 + \nu_4$ may be relaxed by the process

$$CH_4(\nu_2+\nu_4) + CH_4 \rightleftharpoons CH_4(2\nu_4) + CH_4 + 218 \ cm^{-1} \quad (17)$$

$$\longrightarrow CH_4(\nu_4) + CH_4(\nu_2) - 11 \ cm^{-1} \quad (18)$$

$$\longrightarrow CH_4(\nu_4) + CH_4(\nu_4) + 216 \ cm^{-1} \quad (19)$$

V → V equilibration is then completed by

$$CH_4(2\nu_4) + CH_4 \longrightarrow CH_4(\nu_4) + CH_4(\nu_4) - 2 \ cm^{-1} \quad (20)$$

$$CH_4(\nu_2) + CH_4 \rightleftharpoons CH_4(\nu_4) + CH_4 + 227 \ cm^{-1} \quad (21)$$

and finally V → T, R relaxation occurs on a much longer timescale. Endoergic transfers to $CH_4(2\nu_2)$ and $2CH_4(\nu_2)$ have

been neglected. The relaxation is monitored by observing total fluorescence from the ν_4 mode and also the hot fluorescence transmitted through a gas filter. Initially there is one quantum of ν_4 excitation per photon absorbed and all of the fluorescence is hot. After V → V equilibration, conversion of ν_2 quanta to ν_4 and sharing of the excitation among molecules yields 1.64 quanta of "cold" excitation, fundamental fluorescence. Total ν_4 fluorescence increases monotonically toward this limit. The hot ν_4 fluorescence, Fig. 6, increases or decreases initially depending on whether $k_{17} - k_{18} - k_{19}$ is positive or negative. The small initial increase and plateau of hot ν_4 fluorescence shows that k_{17} is slightly larger than $k_{18} + k_{19}$. As $\nu_2 + \nu_4$ equilibrates with $2\nu_4$ at a ratio of 1/3, hot ν_4 fluorescence decays at a rate of

$$0.75\ k_{20} + 0.25(k_{18}+k_{19}) = 0.6 \pm 0.2\ \mu sec^{-1}\ Torr^{-1}.$$

The rate constants for intermolecular transfer of bending quanta k_{20} and $k_{18} + k_{19}$ should be of approximately the same order of magnitude and thus $k_{20} \simeq 0.6\ \mu sec^{-1}\ Torr^{-1}$. From the initial shape of the hot fluorescence curve and from the approximate equalities deduced above we may conclude that

$$k_{17} = 1 \pm 0.5\ \mu sec^{-1}\ Torr^{-1}.$$

E. Summary of rates

Table I gives approximate rates for the various types of V → V energy transfer processes which occur in pure CH_4. All of the rates fall in the range of roughly 0.1 to 1 μsec^{-1} $Torr^{-1}$, or (0.3 to 3) x 10^{-11} cm^3 $molecule^{-1}$ sec^{-1}, corresponding to probabilities per gas kinetic collision between 10^{-2} and 10^{-1}. The scaling factor appropriate for first order perturbations of harmonic oscillators is listed for each measured rate or type of rate. If these V → V transfer rates scale in this way, then the rates for the process involving transitions between levels v = 0 and v = 1 may be found by dividing the reported rate by the factor n. The fastest rate is for transfer of energy within a single molecule between the symmetric and asymmetric stretching modes. The analogous processes for bending vibrations, intramolecular conversion between ν_2 and ν_4 excitation, is also fast. The stretch-to-bend transfers are dominated by intramolecular conversion of ν_3 primarily to $2\nu_4$ and $\nu_2 + \nu_4$. In any case $\nu_2 + \nu_4$ and $2\nu_4$ are rapidly equilibrated. Presumably $2\nu_2$ also equilibrates rapidly with these levels by this rapid intramolecular interconversion of ν_2 and ν_4 quanta. For the stretch-to-bend relaxation of ν_3 it has been observed previously that rare gases are comparably effective to methane itself as energy transfer collision partners. This should be true for all of the intramolecular transfer processes. The intermolecular V → V transfers are slower than the intramolecular ones even

though they involve smaller changes in total vibrational energy. The rates for transfer of a bending or a stretching quantum from one molecule to another are listed at the bottom of Table I.

Recently de Vasconcelos and de Vries[7] have reported spectrophone relaxation measurements on CH_4 and CD_4 in which both ν_3 and ν_4 excitation were used. Their data are completely consistent with the laser fluorescence data presented here and in previous works.[3, 4] They observed relaxation times for overall V → T, R relaxation analyzed by a two-state model of 1.63 ± 0.02 μsec atm for ν_4 excitation and 1.41 μsec atm for ν_3 excitation. When ν_3 is excited, V → V equilibration produces an equilibrated mixture of ν_2 and ν_4 excitation on a timescale two orders of magnitude faster than detectable by acoustic response. The 3019 cm^{-1} ν_3 quantum is transfered to an excitation of $2[(0.82 \cdot 1306) + (0.18 \cdot 1533)] = 2694$ cm^{-1}. Thus the V → V transfer energy discrepancies are deposited instantly as translation-rotation energy and 2694/3019 = 0.89 of the energy is transfered at the V → T, R rate. It is for this reason that the ratio of observed relaxation times $\tau_{\nu_3}/\tau_{\nu_4} = 0.87 \pm > 0.02$. The relaxation mechanism from which de Vasconcelos and de Vries derive a V → V transfer rate of 0.003 μsec^{-1} $Torr^{-1}$ is incorrect.

In conclusion, approximate values are found for the different types of V → V energy transfer processes which relax the higher vibrational levels of methane. In systems which

are only partially relaxed the relative speed of intramolecular processes vs intermolecular ones will tend to keep the excitation energy concentrated in the molecule excited. Thus in experiments such as those of Ehrlich[16] or Yates[17] and their collaborators on gas-surface interactions the population of $CH_4(2\nu_4)$ will be more important than the production of $2CH_4(\nu_4)$ following ν_3 excitation. To the extent that intramolecular transfers are faster than intermolecular ones, laser-induced chemical reactions of small molecules may be favored by keeping the total energy of a molecule above threshold while energy is transfered to the most effective modes for reactions.

ACKNOWLEDGMENTS

We are grateful to Floyd Hovis for his assistance with the experiments. We thank the Air Force Office of Scientific Research and the Division of Chemical Sciences, Office of Basic Energy Sciences, U.S. Department of Energy under contract No. W-7405-Eng-48 for their research support.

REFERENCES

a) Present address: Physikalisch-Chemisches Institut der Universität Heidelberg, Neuenheimer Feld 1, 69 Heidelberg, West Germany

1. K. Fox, Analysis of Vibration-Rotation Spectra of Methane, U.S. Nat'l. Tech. Inform. Serv., AD Rep. 1974, No. 776061/4GA.
2. G. Herzberg, Molecular Spectra and Molecular Structure II, Infrared and Raman Spectra of Polyatomic Molecules (Van Nostrand, Princeton, 1945).
3. J.T. Yardley and C.B. Moore, J. Chem. Phys. 49, 1111 (1968).
4. P. Hess and C.B. Moore, J. Chem. Phys. 65, 2339 (1976).
5. T.L. Cottrell and A.J. Matheson, Trans. Faraday Soc. 58, 2336 (1962).
6. M. Huetz-Aubert, F. Lepoutre, and G. Louis, J. Phys. 38, 283 (1977).
7. M.H. de Vasconcelos and A.E. de Vries, Physica 86 A, 490 (1977).
8. P.F. Zittel and C.B. Moore, J. Chem. Phys. 58, 2004 (1973).
9. S.R. Leone and C.B. Moore, Chem. Phys. Lett. 19, 340 (1972).
10. J. Finzi and C.B. Moore, J. Chem. Phys. 63, 2285 (1975).
11. S.J. Brosnan and R.L. Byer, IEEE J. Quantum Electron. QE-15, 415 (1979).

12. J.T. Yardley, M.N. Fertig, and C.B. Moore, J. Chem. Phys. 52, 1450 (1970).

13. D.H. Rank, D.P. Eastman, G. Skorinko, and T.A. Wiggins, J. Mol. Spectrosc. 5, 78 (1960).

14. W.L. Barnes, J.Susskind, R.H. Hunt, and E.K. Plyler, J. Chem. Phys. 56, 5160 (1972).

15. R.H.Hunt, L.R. Brown, and R.A. Toth, J. Mol. Spectrosc. 69, 482 (1978).

16. S.G. Brass, D.A. Reed, and G. Ehrlich, J. Chem. Phys. 70, 5244 (1979).

17. J.T. Yates, Jr., J.J. Zinck, S. Sheard, and W.H. Weinberg, J. Chem. Phys. 70, 2266 (1979).

TABLE I. Rates of collisional V → V energy transfer in CH_4 at 294 K.

	n[a]	$(p\tau)^{-1}$ (μsec^{-1} $Torr^{-1}$)	k x 10^{11} (cm^3 $molec^{-1}$ sec^{-1})	P[b]
		Processes predominantly intramolecular		
$\nu_3 \leftrightarrow \nu_1$	1	$k_1 = 1.2 \pm 0.3$	3.6	0.09
$\nu_2+\nu_4 \leftrightarrow 2\nu_4$	2	$k_{17} = 1 \pm 0.5$	3	0.08
$\nu_3 \rightarrow 2\nu_b$	1	$k'_9 = 0.28 \pm 0.06$	0.8	0.022
$2\nu_3 \rightarrow \nu_3+2\nu_b$	2	$k'_{12}+k'_{13} = 0.6 \pm 0.2$	1.8	0.05
$\nu_3+\nu_4 \rightarrow 3\nu_b$	1-2	$k'_8 = 0.7 \pm 0.2$	2.1	0.05
		Intermolecular single quantum transfer		
ν_4	2	$k_{20} = 0.6 \pm 0.2$	1.8	0.05
stretch	2	$k'_{11}+2k'_{14} = 0.25 \pm 0.15$	0.8	0.02
bend and strech	1	$k'_2 = 0.2 \pm 0.1$	0.6	0.02

a. Normalization factor for first order perturbation of harmonic oscillators

b. Probability per gas kinetic collision, $(p\tau Z)^{-1}$, Ref. 4.

Figure 1. Energy levels of CH_4 with laser excitation (⟶) and some fluorescence (⇝) transitions indicated.

Figure 2. Decay of ν_3 fluorescence following overtone and combination level excitation. Reciprocal lifetime versus pressure for the fall of hot ν_3 fluorescence, $p\tau$ = 1.2 ± 0.3 μsec Torr (open symbols) and for the fall of fundamental ν_3 fluorescence, $p\tau$ = 3.3 ± 0.7 μsec Torr (solid symbols): △, ▲ excitation of $2\nu_3$; ○, ● excitation of $\nu_3 + \nu_4$; □, ■ excitation of $\nu_1 + \nu_4$.

Figure 3. V → V transfer $\nu_3 \leftrightarrow \nu_1$. Reciprocal lifetime versus pressure for the rise of hot ○, total ▲, and fundamental □ ν_3 fluorescence exciting the combination band $\nu_1 + \nu_4$. The slope drawn is 1.8 μsec^{-1} $Torr^{-1}$.

Figure 4. Stretch-to-bend relaxation. Reciprocal lifetime versus pressure for the fall of total ν_3 fluorescence: ○ excitation of P(9) of the fundamental ν_3; △ excitation of P(8) (ν_3) in $^{13}CH_4$ (sample 10% $^{12}CH_4$ and 90% $^{13}CH_4$; ● excitation of P(6) of the fundamental ν_3; ▲ excitation of P(5) ν_3 in $^{13}CH_4$. The decay time for CH_4 is 3.2 ± 0.6 μsec Torr and for $^{13}CH_4$ 3.5 ± 0.6 μsec Torr.

Figure 5. V → V transfer among bending levels. Reciprocal lifetime vs pressure for: rise of total (●) and hot (○) ν_4

fluorescence after ν_3 Q-branch excitation; and fall of hot ▲ ν_4 fluorescence after $\nu_2 + \nu_4$ excitation. The slopes are 0.31 and 0.55 μsec^{-1} $Torr^{-1}$.

Figure 6. Hot ν_4 fluorescence intensity vs time following $\nu_2 + \nu_4$ excitation at 1.11 Torr. Beyond 2 μsec the decay time is 1.5 μsec. The electronics response time has been increased to 0.3 μsec. S/N is the lowest of all data used in this work.

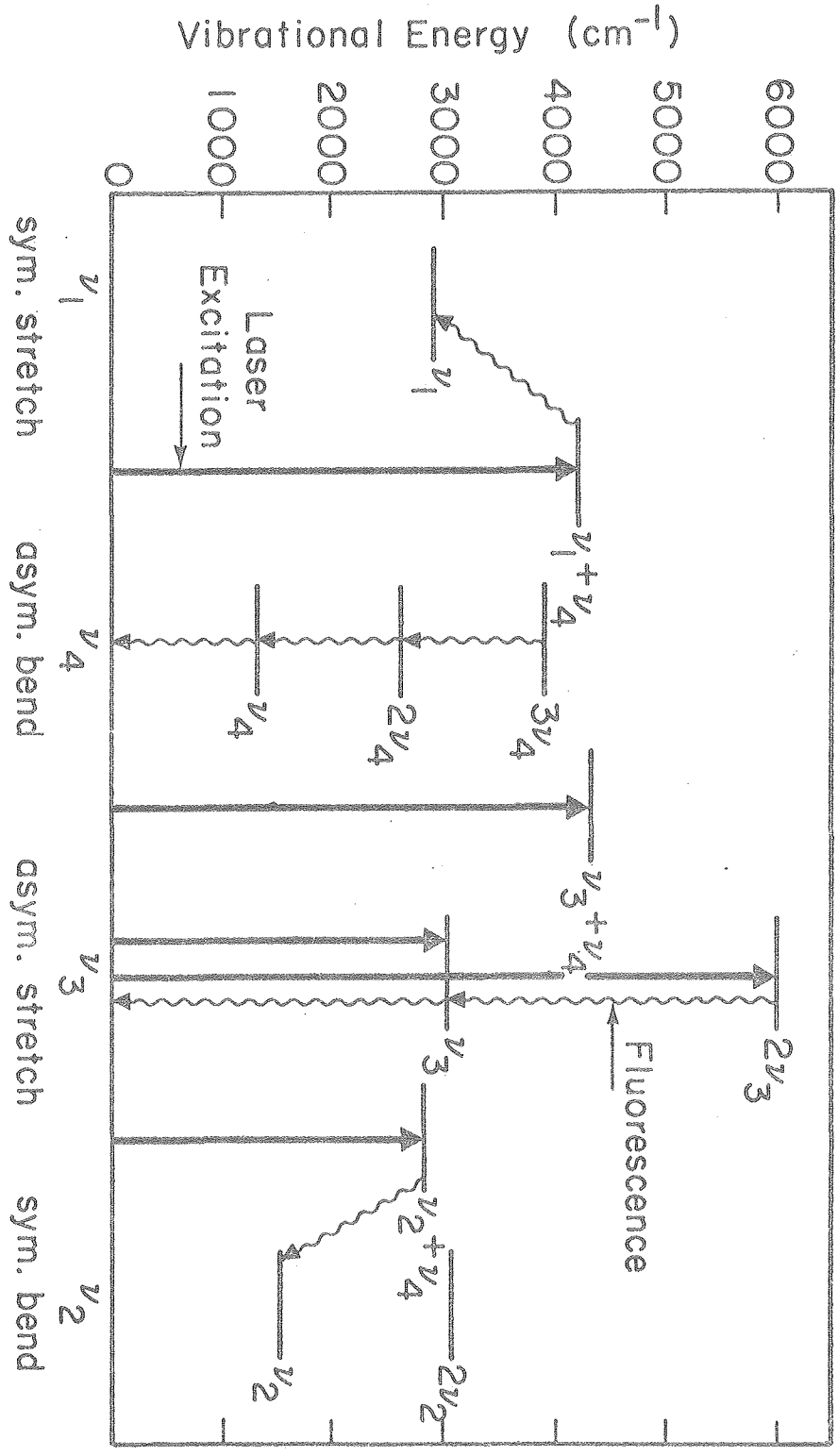
Vibrational Energy (cm⁻¹)
0
1000
2000
3000
4000
5000
6000
sym. stretch
asym. bend
asym. stretch
sym. bend
Laser Excitation
Fluorescence
ν1
ν1+ν4
ν4
2ν4
3ν4
ν3+ν4
2ν3
ν3
ν2+ν4
2ν2
ν2

XBL 787-9565

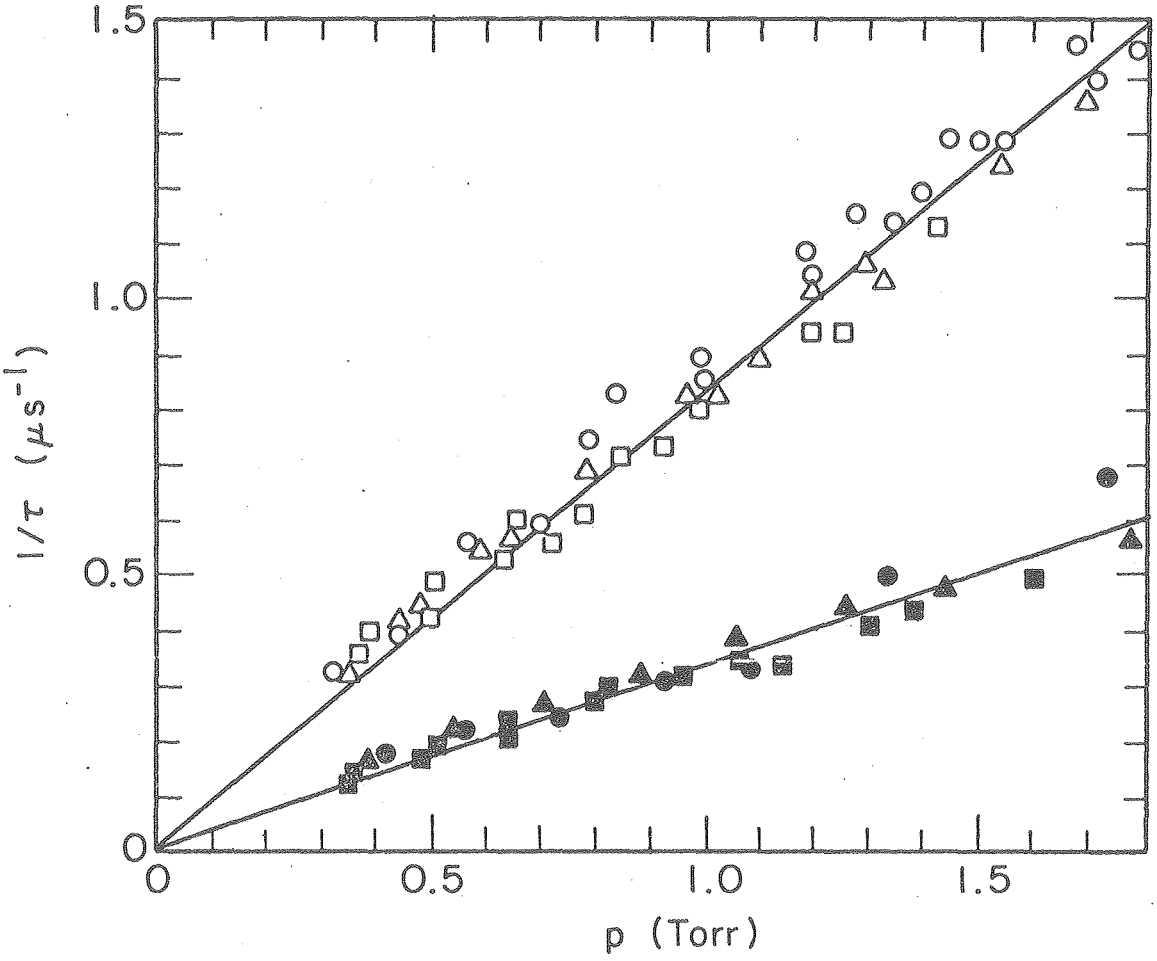

XBL 787-9564

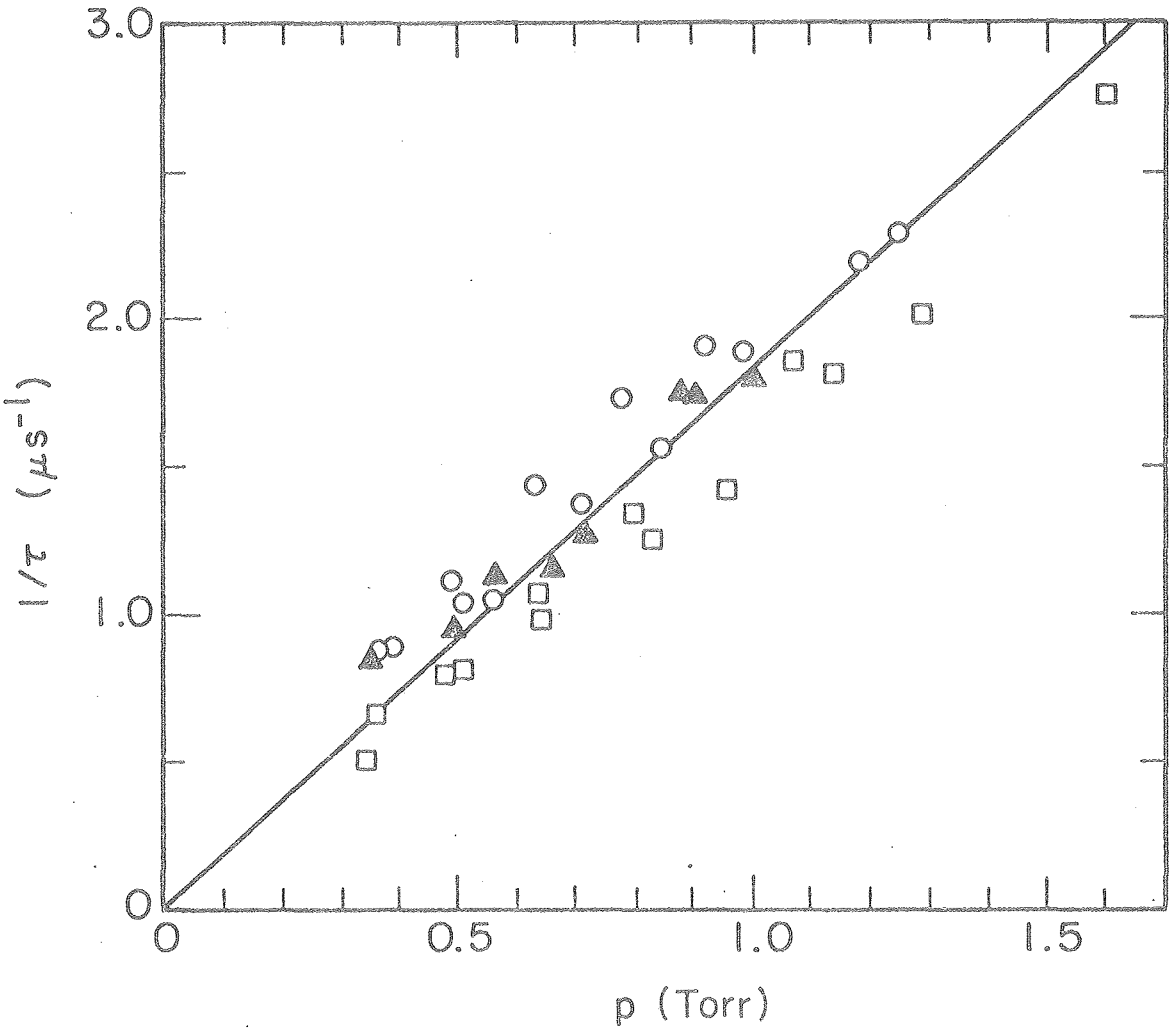

XBL 787-9563

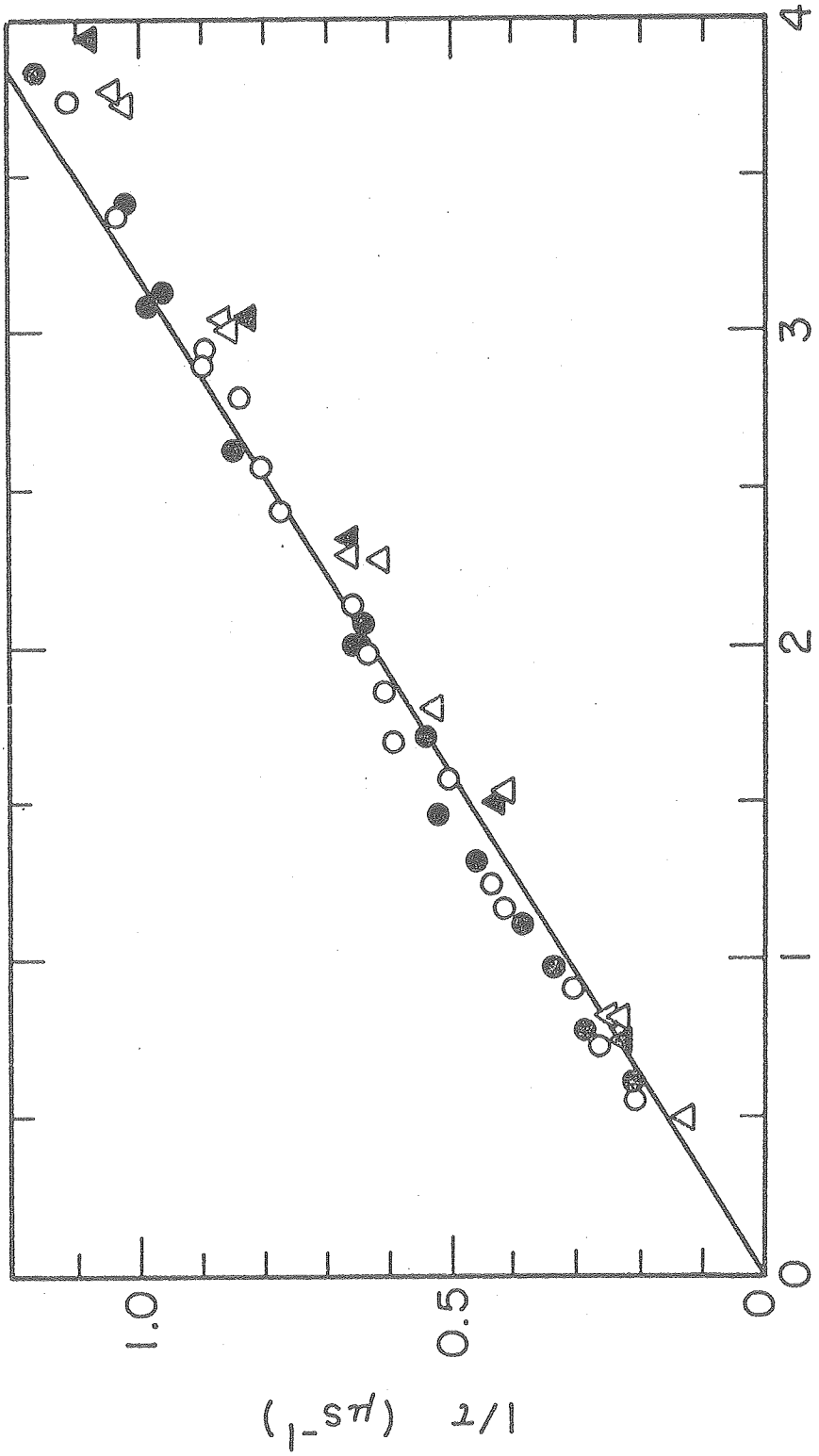

XBL 787-9552

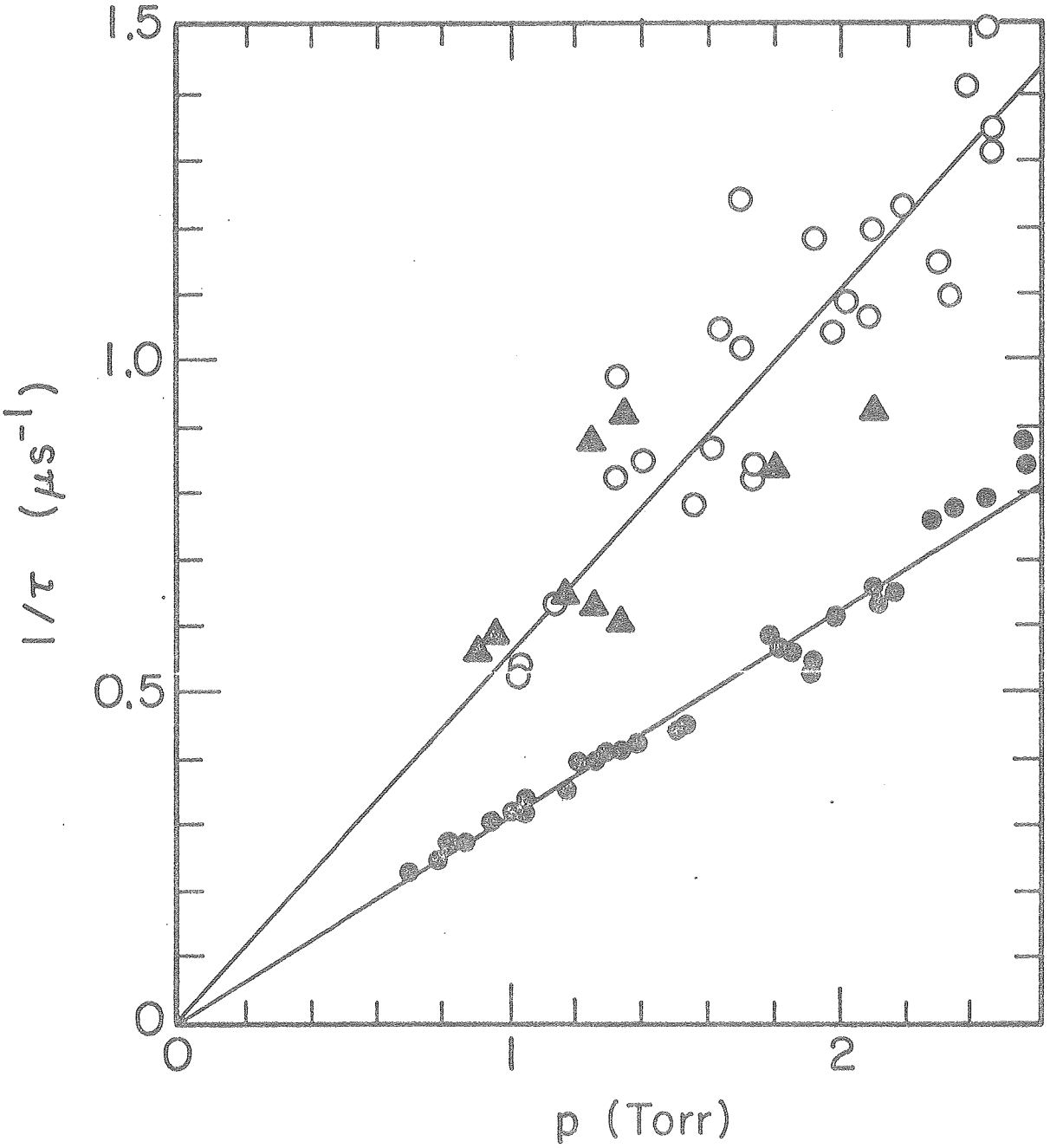

XBL 787-9556 A

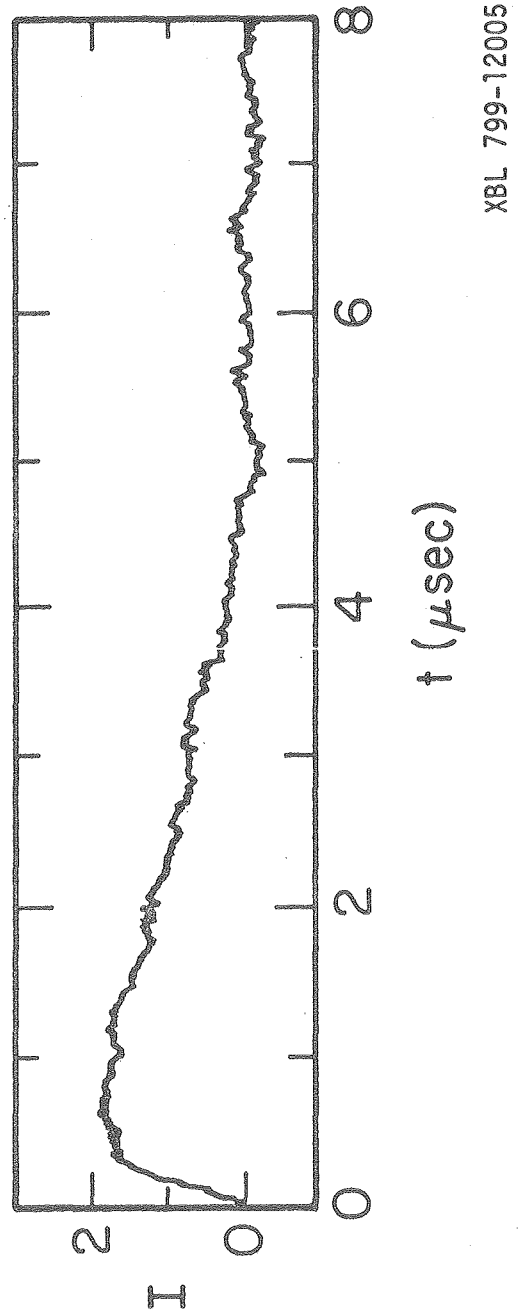

XBL 799-12005